Multiphysics Time-Domain Modeling of Nonlinear Permeability in Thin-film Magnetic Material

Zhi Yao[1], Han Cui[1], Tatsuo Itoh[1] and Yuanxun Ethan Wang[1]
[1]University of California, Los Angeles, USA

***Abstract*— A fast-converging one-dimensional (1-D) finite-difference time-domain (FDTD) algorithm has been proposed based on reduction strategy of unknowns in electromagnetic (EM) fields. The proposed algorithm solves simultaneously Maxwell's equations and Landau-Lifshitz-Gilbert (LLG) equation with nonlinear effects. Therefore, the proposed algorithm can predict the dynamic interaction between magnetic spins and EM fields. The accuracy of the modeling has been validated by 1. a standard magnetic switching process under static magnetic fields, and 2. the dispersive permeability of a PEC-backed continuous ferrite film with a 3 μm-thickness, under dynamic electric excitation. The simulated permeability agrees with the theoretical prediction, under both linear and nonlinear circumstances. Specifically, the algorithm has fully revealed numerically that sufficiently large RF power can decrease the ferromagnetic resonance (FMR) frequency and suppress the permeability.**

***Index Terms*— electromagnetics, ferrite, ferromagnetic, finite difference time domain methods, magnetics, multiphysics, nonlinear problems, thin films**

I. Introduction

Magnetic materials are intrinsically nonlinear, dispersive, non-reciprocal and anisotropic [1]-[3] in microwave regime even within the framework of classical micromagnetics described by the Landau-Lifshitz-Gilbert (LLG) theory. Specifically, the nonlinearity and dispersion, especially in film shape, can be utilized to create frequency selective limiters (FSL) [4, 5] or signal to noise enhancers (SNE) [6] that can operate in an RF front-end. In order to improve materials on a systematic basis, it is essential to build modeling tools for design and optimization [7], which eliminate much of the expense in constructing magnetic devices. The modeling tool must include accurate description of the coupling between the dynamic magnetization and the electromagnetic (EM) field, and can show how devices are likely to perform. However, the state of the art in modeling RF magnetic components is significantly lagging that in modeling components consisting of only electric material, with most commercial RF design software limited to linear material behavior. In addition, the dramatic scale difference between the film thickness and EM wavelength cannot be adequately addressed with commercial software due to the overwhelming computational complexity in both space and time gridding.

This work proposes a one-dimensional (1-D) time-domain multiphysics modeling algorithm, which solves electrodynamics and nonlinear spin dynamics interactively. Section II elaborates the formulation of the modeling. The modeling is based on reduction strategy of unknowns in EM fields to overcome the stability issue. Magnetization at the interface between the magnetic film and air is handled with 1-D demagnetization. In Section III, two numerical examples have demonstrated the accuracy and efficiency of the proposed method. In III. A, an exemplary magnetic switching process demonstrates the nonlinear behavior of magnetization under static magnetic field. Section III. B serves as description of the coupling between the dynamic magnetization and the electromagnetic (EM) fields. The simulated permeability agrees with the theoretical prediction, under both linear and nonlinear circumstances. Specifically, the algorithm has fully revealed that sufficiently large RF power can decrease the ferromagnetic resonance (FMR) frequency and suppress the permeability.

II. FDTD with Nonlinear Spin Dynamics

In the multiphysics problem involving ferromagnetic RF devices, dynamic Maxwell's equations and LLG equation should be considered, shown respectively as the following:

$$\nabla \times \boldsymbol{H} = \epsilon \frac{\partial \boldsymbol{E}}{\partial t} + \boldsymbol{J} + \sigma \boldsymbol{E}, \nabla \times \boldsymbol{E} = -\frac{\partial \boldsymbol{B}}{\partial t}, \tag{1}$$

$$\frac{\partial \boldsymbol{M}}{\partial t} = \mu_0 \gamma (\boldsymbol{M} \times \boldsymbol{H}) - \frac{\alpha \mu_0 \gamma}{|\boldsymbol{M}|} \boldsymbol{M} \times (\boldsymbol{M} \times \boldsymbol{H}), \tag{2}$$

where the gyromagnetic ratio is $\gamma = -1.759 \times 10^{11} C/kg$, and the magnetic damping constant is $\alpha = -\mu_0 \gamma \Delta H / 4\pi f_r$, with ΔH being the FMR linewidth and f_r the FMR frequency. The pictorial representation of (2) is shown in Fig. 1.

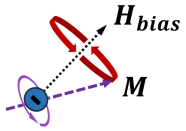

Fig. 1. Electron angular momentum (called spin) leads to a magnetic moment $\boldsymbol{M}$ precessing around the applied magnetic field $\boldsymbol{H}_{bias}$, resulting in the coupling between magnetic field components transverse to the bias.

A. Formulation of Coupled Differential Equations

The nonlinear phenomenon favors time-domain representation, therefore, finite-difference time-domain method is used. Even in 1-D simplification, the modeling suffers the three challenges introduced in [8], especially in nonlinear cases. Firstly, the algorithm should solve (1) and (2) in a simultaneous manner, due to strong coupling of magnetization to the EM field. Secondly, one needs to resolve the stability issue, because LLG equation requires a drastically smaller spatial scale than the EM wavelength. Moreover, the nonlinear be-

havior exacerbates this challenge. Finally, demagnetization should be incorporated. The first two challenges are overcome by concurrently solving (1) and (2) with EM field unknown reduction, while the third one by rigorous analysis of the boundary conditions and instantaneous EM field coupling with magnetic spin.

Without loss of generality, apply a magnetic DC bias field H_i in the y direction, to saturate the magnetic material so that it presents magneto-dynamic properties and the magnetization magnitude equals to M_S. Equation (2) can be reduced into the nonlinear scalar form as:

$$\frac{\partial M_x}{\partial t} = \mu_0\gamma[M_yH_z - M_z(H_y + H_0)] - \frac{\alpha\mu_0\gamma}{M_S}\{M_x[M_y(H_y + H_0) + M_zH_z] - M_y^2H_x - M_z^2H_x\}, \quad (3)$$

$$\frac{\partial M_y}{\partial t} = \mu_0\gamma[-M_xH_z + M_zH_x] + \frac{\alpha\mu_0\gamma}{M_S}\{M_y[M_xH_x + M_zH_z] - M_x^2(H_y + H_0) - M_z^2(H_y + H_0)\}, \quad (4)$$

$$\frac{\partial M_z}{\partial t} = \mu_0\gamma[M_x(H_y + H_0) - M_yH_x] - \frac{\alpha\mu_0\gamma}{M_S}\{M_z[M_xH_x + M_y(H_y + H_0)] - M_x^2H_z - M_y^2H_z\}, \quad (5)$$

with $H_{x,y,z}$ being the dynamic field components and $M_{x,y,z}$ being the total magnetization components.

Under nonlinear circumstances, the time-step size of a converging FDTD algorithm is orders of magnitude smaller than that in linear cases, i.e. Courant-Friedrichs-Lewy (CFL) limit is not strict enough to determine the time step. However, a time-step size that is much smaller than the RF cycle would lead to severe oversampling and poor computational efficiency. To avoid the oversampling issue, one may use a much sparser grid than the device size, to describe its spatial behavior and then interpolate the electromagnetic field inside the large grid with polynomial basis functions. This leads to the reduction in the number of unknowns for electromagnetic field variables and avoids the stability problem or oversampling problem. However, such method requires prior knowledge of the simulated structures. Specific to the 1-D FDTD algorithm implemented for thin film structures backed by perfect electric conductor (PEC), a single grid is needed to represent the electromagnetic field unknowns in the magnetic material and the following polynomial spatial expansion of electromagnetic field is used to derive the field on the thin film grid:

$$H_x = H_{x0}, M_x = M_{x0}, E_y = E_{y1}z \quad (6)$$

where H_{x0}, M_{x0}, E_{y1} are unknowns to be solved by 1-D FDTD. The E_y field has approximated linear distribution in the film thickness direction due to the fact that electric field is zero on PEC and monotonically increasing away from the PEC. Field components H_{y0}, M_{y0} and E_{x1} can be constructed similarly. If more dramatic electromagnetic field variation is expected, higher order terms could be added to (6) for better accuracy. The radiation boundary condition takes the form,

$$\left.\frac{E_y}{H_x}\right|_{z=d} = -\eta_0, \quad (7)$$

which together with (1) yield

$$\frac{\partial B_x}{\partial t} = -\frac{\eta_0}{d}H_{x0}. \quad (8)$$

Similarly,

$$\frac{\partial B_y}{\partial t} = -\frac{\eta_0}{d}H_{y0} \quad (9)$$

The 1-D boundary condition leads to a demagnetization field of

$$H_z = -M_z \quad (10)$$

B. Flow of 1-D FDTD

A straightforward discretization of (3)-(5), (8)-(10) and the magnetic constitutive relations yields the time-difference equations for FDTD simulation. The flow of the FDTD time-marching is illustrated as the following:

Step 1: Update $M_{x,y,z}^{n+1}$ using discretized (3)-(4);

Step 2: Update $B_{x,y}^{n+1/2}$ using discretized (8) and (9);

Step 3: Update $H_{x,y,z}^{n+1}$ using constitutive relation and (10). Note (10) only applies to thin film geometry;

Step 4: Normalize the magnitude of magnetization by the saturation magnetization to meet the angular rotation condition as indicated in Fig. 1. The mathematical form of this step is $M_{x,y,z} = M_{x,y,z} \cdot (|M|/M_S)$.

Step 1-3 can be conducted in either forward time sequence or temporal extrapolation to calculate the unknown field components. For example, the calculation of M_x^{n+1} requires the knowledge of $M_y^{n+1/2}$, which is unknown. One can assume $M_y^{n+1/2} \approx M_y^n$ with refined time steps, or extrapolate the unknown by $M_y^{n+1/2} \approx (3M_y^n - M_y^{n-1})/2$.

III. Numerical Validation

Two numerical examples will be presented in this section. The first example represents the magnetization switching process. It demonstrates the nonlinear behavior of magnetization under static magnetic field. The second example predicts the underlying physics of the relationship between EM fields and properties of magnetic materials. It demonstrates the nonlinear behavior of dynamic magnetization interacting with EM field.

A. Magnetization Switching

The first validation example resembles a simplified version of the μMag standard problem # 4 [9] in the 1-D form, representing the magnetization switching process. The magnetic material is assumed to fill up the half space on one side of the PEC. The magnetic spin is initialized in the x direction. At $t = 10\ ns$, a magnetic DC bias field $H_0 = 20\ Oersted$ is applied in y direction. The saturation magnetization is set to be that of yttrium-iron-garnet (YIG), i.e. $4\pi M_S = 1750\ [Gauss]$. In Fig. 2(a), the damping constant α is set to be an artificially large value of -0.5, so that the spin quickly reaches static condition.

However, in reality, the damping constant of YIG is on the order of 10^{-3}, as in Fig. 2(b). The spin resonates in the mean-time of damping, at the FMR frequency $f_0 = \mu_0 \gamma H_0 / 2\pi$.

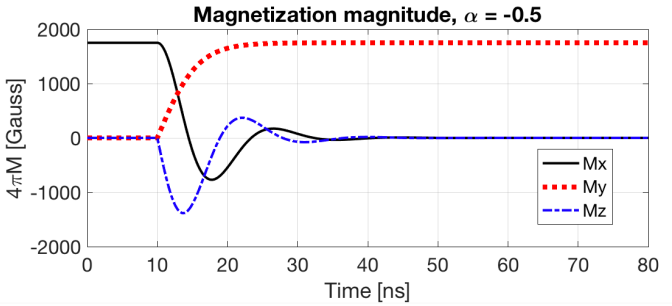

(a)

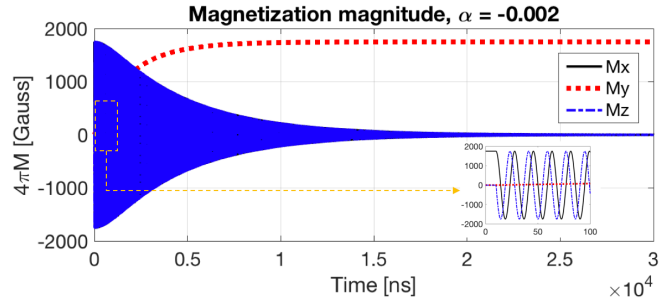

(b)

Fig. 2. Magnetic switching process. The magnetic spin is reoriented at $t = 10\ ns$ from x direction to y direction by a magnetic DC bias in the y direction with the value of 20 Oersted. (a) $\alpha = -0.5$, (b) $\alpha = -0.002$.

B. Linear and Nonlinear Permeability

A thin film of YIG backed by a PEC ground, with infinite planar dimensions and a 3-μm thickness, is assumed. A continuous current sheet is placed on top of the thin film shown by Fig. 3, with various magnitudes. The time-step is $1/10^5$ of the RF cycle ($\Delta t = 1.4584 \times 10^{-14} s$). The surface current excitation is a continuous dynamic wave $J_{sy} = \cos(\omega t)$, with ω sweeping over the frequency range of interest. The realistic properties of YIG are applied to the magnetic thin film, i.e. $4\pi M_S = 1750\ [Gauss]$, $\epsilon_r = 13$, $\sigma = 0$, $\Delta H = 2\ [Oersted]$. The thin film is magnetized by an in-plane DC magnetic bias ($H_0 = 80\ Oersted$) parallel to the electric current excitation, so that the FMR frequency is near 1.07 GHz, according to Kittel's equation [3]. The initial orientation of magnetic spin is in y direction.

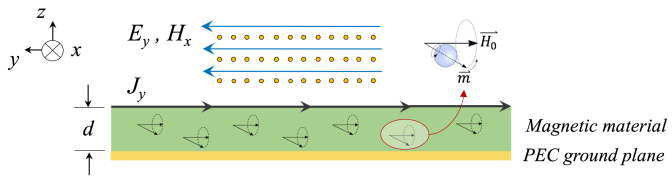

Fig. 3. Infinite YIG thin film backed by PEC ground, on which a uniform electric current sheet is placed. $\mu_r k_0 d \ll 1$.

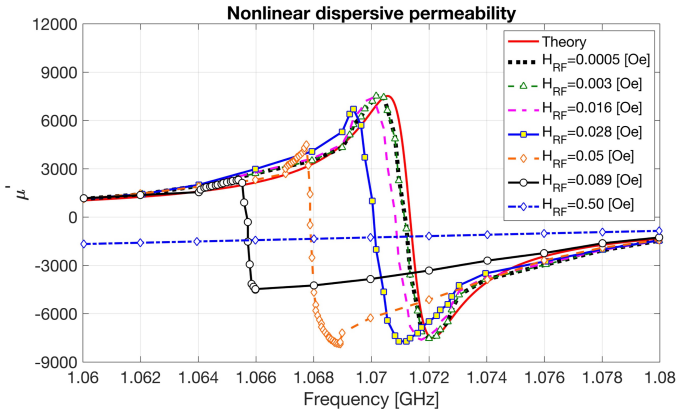

(a)

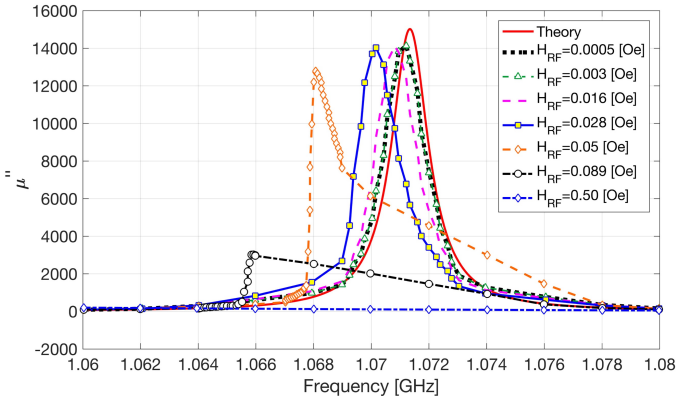

(b)

Fig. 4. Dispersive permeability simulated with the structure in Fig. 3. (a) real part μ', (b) imaginary part μ''.

As can be seen in Fig. 4, when the excited RF magnetic field is low, the simulated permeability matches with the theory based on small signal perturbation [3]. This agreement validates the proposed method in the linear region. When the RF field increases to be larger than $0.016\ [Oersted]$, the FMR frequency down-shifts due to lower M_y. In addition, the dispersive permeability suffers peak value suppression and linewidth broadening as the RF field further increases. This phenomenon has been experimentally discovered by the magnetics society [3]. The simulated nonlinear permeability can demonstrate the potential of the proposed modeling for design of nonlinear devices such as FSL. Further investigation of the nonlinear magnetics requires consideration of spin waves, which is under progress.

IV. Conclusion

A multiphysics modeling technique based on 1-D FDTD is proposed, to accurately model the dynamic interaction between nonlinear spin dynamics and electrodynamics. The proposed method provides clearer understanding on the role of nonlinear magnetics in RF devices compared to existing micromagnetics solvers and EM simulators. With further extension into 3-D unconditionally stable algorithm, such as alternating-direction-implicit (ADI) FDTD [10], one is able to in-

clude magneto-crystalline anisotropy, exchange coupling and spin transfer torque. Therefore, the proposed algorithm can be potentially used to design realistic nonlinear RF magnetic and spintronic devices.

REFERENCES

[1] M. Wu, A. Hoffmann, et al., *Solid State Physics*, vol. 64, Eds., ed: Academic Press, 2013, Elsevier, 2013.

[2] V. G. Harris, "Modern Microwave Ferrites," *IEEE Trans. Magnetics*, vol. 48, no. 3, pp. 1075-1104, Mar. 2012.

[3] B. Lax and K. J. Button, *Microwave Ferrites and Ferrimagnetics*, McGraw-Hill, New York, 1962.

[4] H. Suhl, "The nonlinear behavior of ferrites at high microwave signal levels," *Proceedings of the IRE*, vol. 44, no. 10, pp. 1270-1284, Oct. 1956.

[5] R. W. Orth, "Frequency-selective limiters and their application," *IEEE Trans. Electromagn. Compat.*, vol. EMC-10, no. 2, pp. 273-283, Jun. 1968.

[6] J. D. Adam and S. N. Stitzer, "A magnetostatic wave signal-to-noise enhancer," *Applied Physics Letters*, vol. 36, no. 6, pp. 485-487, Mar. 1980.

[7] H, Kronmuller and S. Parkin, *Handbook of Magnetism and Advanced Magnetic Materials*, Wiley, 2007.

[8] Z. Yao and Y. E. Wang, "3D unconditionally stable FDTD modeling of micromagnetics and electrodynamics." Microwave Symposium (IMS), 2017 IEEE MTT-S International, pp. 12-15. IEEE, 2017.

[9] R. D. McMichael, et al. "Switching dynamics and critical behavior of standard problem No. 4." Journal of Applied Physics 89.11 (2001): 7603-7605.

[10] F. Zheng, Z. Chen and J. Zhang, "Toward the development of a three-dimensional unconditionally stable finite-difference time-domain method," *Microwave Theory and Techniques, IEEE Transactions on*, vol. 48, vol. 9, pp. 1550-1558, Sep. 2000